Journal Name

ARTICLE TYPE

Synthesis and Self-Assembly of a Novel Fluorinated Triphilic Block Copolymer

Xinxin Li*[a], Yanhua Yang[a], Guojun Li[a] and Shaoliang Lin*[ab]

A novel fluorinated diblock tercopolymer was synthesized by the reversible addition fragmentation chain transfer method, incorporating methacrylic acid, methyl methacrylate, and perfluoroalkyl ethyl methylacrylate blocks as hydrophilic, lipophilic, and fluorophilic units, respectively. Depending upon the specific triphilic balance, by control solution conditions, the block copolymer self-assembled in
10 dimethylformamide/water dispersions induced an evolution from spheres to wormlike structures, finally to novel nail-shaped structures, as verified by transmission electron microscopy and dynamic light scattering. The control mechanism is explained in terms of the effect of each property on the forces that govern the formation of any given morphology, namely the core-chain stretching, strong incompatibility between the lipophilic blocks and the fluorophilic blocks, and interfacial tension.

15 Introduction

The shape of polymer micelles is important for pharmaceutical applications as drug delivery. The hydrophobic blocks of the copolymer are segregated to form the inner core that can encapsulate poorly water-soluble drugs, and the hydrophilic
20 blocks form the corona or outer shell that makes the micelle water-soluble. Therefore, polymeric micelles have long been well recognized as excellent candidates for drug delivery carriers.[1-3] Synthetic polymers incorporating fluorine segments or blocks and their aggregation behavior in selective solvents are highly
25 interesting for biomedical and pharmaceutical research due to the singular biological activity imparted by the fluorinated moieties.[4-6] Recently, block copolymers with three mutually incompatible segments, therefore the term "triphilic" is used occasionally,[6, 7] have become easily accessible, thanks to alternative and other
30 controlled radical polymerization techniques.[7-10]

The triphilic copolymers self-assembly in solution have so far produced core-shell-corona systems,[9, 11, 12] multicompartmental micelles,[9, 12-19] raspberry,[20] soccer ball,[9, 12] hamburger structures,[21] micelles with segregated coronas,[9] core-
35 compartmentalized micelles,[15, 16, 21] and numerous other systems,[16, 17, 22] thus rendering them most interesting objects for

fundamental studies. The morphologies of the aggregates are controlled by a force balance involving core chain stretching, interfacial energy between the core and the solvent, repulsion
40 between corona chains, volume fraction of each block, and the Flory-Huggins interaction parameter (χ) between core and corona chains.[23] Whereas the self-assembly of amphiphilic block copolymers in aqueous solution into a wealth of colloidal aggregates have been investigated intensely,[24-30] studies on the
45 self-assembly of triphilic block copolymers containing a fluorocarbon block are much less common. To the best of our knowledge, except some reports from a few research groups,[9, 12, 14-18, 20, 21, 31] only a few examples have been reported,[32-37] backed up by some theoretical studies and modeling to elucidate the
50 influence of molecular architecture, block length, and polymer concentration on the micellar morphology. However, the procedures were more complex and the reaction conditions were more demanding. For example, Mays *et al*.[32] reported an asymmetrical self-assemble structure obtained from sulfonated
55 polystyrene-*b*-fluorinated polyisoprene (*s*PS-*b*-*f*PI), which was first synthesized by anionic polymerization, followed by fluorination and partially sulfonation. Li *et al*.[38] used two successive anionic polymerization steps, a hydrogenation step and a coupling reaction, in order to prepare *μ*-
60 (poly(ethylethylene))(poly(ethylene oxide))(poly(perfluoropropylene oxide)) miktoarmstar block copolymers. The same group observed later by cryo-TEM the complexity of multicompartment structures formed in dilute aqueous solutions.[15, 17, 31, 39] Nonetheless, the synthesis of these
65 structures was painstaking,[40] and the strategy can be hardly generalized to blocks of other chemical nature. To further explore the relationships between structures and properties, the syntheses of triphilic copolymer in a facile way are much desired.

[a]Key Laboratory of Specially Functional Polymeric Materials and Related Technology of the Ministry of Education, School of Materials Science and Engineering, East China University of Science and Technology, Shanghai 200237, China, Email: xinxinli@ecust.edu.cn
[b]Shanghai Key Laboratory of Advanced Polymeric Materials, School of Materials Science and Engineering, East China University of Science and Technology, Shanghai200237, China, Email: slin@ecust.edu.cn
† Electronic supplementary information (ESI) available: TEM images for worm-like aggregates and nail-shaped aggregates. See DOI: 10.1039/b000000x/
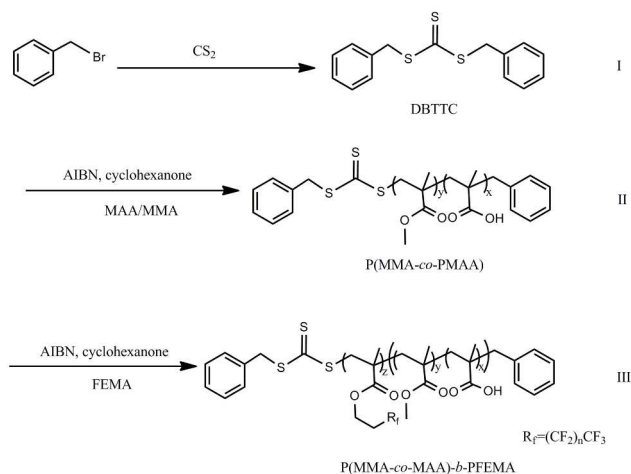
Scheme 1 Synthesis of DBTTC (I), P(MMA-*co*-MAA) (II) and P(MMA-*co*-MAA)-*b*-PFEMA (III).

Herein, we report the synthesis and self-assembly of a specifically designed linear triphilic block copolymer, poly(methylmethacrylater-*co*-methacrylic acid)-*block*-polyperfluoroalkyl ethyl methylacrylate P(MMA-*co*-MAA)-*b*-PFEMA, where PMMA and PMAA were randomly arranged, PMAA is hydrophilic, PMMA is lipophilic and PFEMA is fluorophilic. Hydrocarbon and fluorocarbon blocks were selected since such segments tend to be strongly incompatible and should thus favor the segregation into distinct domains.[41] The synthetic route is shown in Scheme 1. The copolymer was prepared by a facile approach, a two-step reversible addition fragmentation transfer (RAFT) polymerization, using dibenzyltrithiocarbonate (DBTTC) as a chain-transfer agent. Triphilic copolymers with similarly structures were seldom found and used in the self-assembly system. The self-assembly behavior of the copolymer in DMF/H$_2$O dispersion media was carried out by tailoring the water content. It was found that the morphology transition from spheres to wormlike structures, to tapered worms, and finally to novel nail-shaped structures was obtained with the addition of water.

Experimental section

Materials

Methyl methacrylate (MMA, Sinopharm, 98%) was washed with 10%wt NaOH solution three times and then washed with deionized water until neutral, was purified by distillation under reduced pressure at 60 °C in order to remove the inhibitor and oligomer impurities. Methacrylic acid (MAA, Sinopharm, 98%) was distilled under vacuum and then dried with molecular sieves. Perfluoroalkyl ethyl methylacrylate (FEMA, DuPont, AR), with structural formula CH$_2$=C(CH$_3$)COOCH$_2$CH$_2$(CF$_2$)$_n$CF$_3$, mainly n=7~9, different chain length of a mixture of homologues, average n=7.44, the average molecular weight of 554, washed by 10%wt NaOH solution three times to remove inhibitor and then dried with CaH$_2$, filtered and then in the low-temperature sealing preservation. 2, 2'-azobisisobutyronitrile (AIBN, Aldrich, 98%) was recrystallized from methanol. Cyclohexanone was purified and distilled under reduced pressure. Dibenzyltrithiosulfate carbonate (DBTTC) was synthesized as described in the literature,[42] as shown in Scheme 1(I), ^{1}H NMR (400 MHz, CDCl$_3$) δ(ppm): 4.55 (s, 4 H), 7.20-7.27 (m, 10 H). Other reagents and solvents were used without further purification.

Synthesis of P(MMA-*co*-MAA) macroinitiator

The synthesis of P(MMA-*co*-MAA) proceeded by an RAFT approach using DBTTC as chain transfer agent, with the molar ratio of component [MMA/MAA] : [DBTTC] : [AIBN] =200 : 1 : 0.1, [MMA] : [MAA]=5 : 1, as shown in Scheme 1(II). A dry round-bottomed flask with a magnetic stir bar was charged with DBTTC (0.054 g, 1.85×10^{-4} mol), AIBN (0.003 g, 1.85×10^{-5} mol), MMA (3 g, 3×10^{-2} mol), MAA (0.6 g, 7×10^{-3} mol) and cyclohexanone (20 g). The mixture was degassed through three freeze-pump-thaw cycles. The polymerization was carried out at 80 °C for 48 h. The polymer was precipitated into an excess of cyclohexane and dried under vacuum at 60 °C overnight.

Synthesis of P(MMA-*co*-MAA)-*b*-PFEMA

A dry round-bottomed flask with a magnetic stir bar was charged with P(MMA-*co*-MAA) (3 g), AIBN (0.004 g, 1.85×10^{-5} mol), FEMA (0.420 g, 7.8×10^{-4} mol) and cyclohexanone (20 g). The mixture was degassed through three freeze-pump-thaw cycles. The polymerization was carried out at 80 °C for 48 h. The polymer was precipitated into an excess of cyclohexane and dried under vacuum at 60 °C overnight.

Turbidity measurements (OD)

The onset of self-assembly and the subsequent morphological transitions are usually followed by measuring the turbidity of the solution as a function of water content.[43] Turbidity diagrams were constructed according to the following procedure. The triphilic copolymer was first dissolved into DMF, which is a good solvent for the PMMA and PMAA blocks, at a concentration of 1.0 g L^{-1}. Deionized water was then added drop by drop (8 μL per drop to 2 mL of polymer solution) under magnetic stir. After every addition of water, the solution was stirred for 1 min and then left to equilibrate for 3 min or more until the optical density was stable. The optical density (turbidity) was measured by UV-Vis spectrophotometer (UV-2550 SHIMADZU) at a wavelength of 690 nm (which was far from the absorption of the polymer chromophore) using a quartz cell (path length: 1 cm).

Preparation of the self-assembled objects

To prepare the copolymer micelles, deionized water was dropwise added into a dilute DMF solution of polymer at 1.0 g L^{-1} under stirring to give the dispersions at the water content (WC, WC is the water/DMF volume ratios) of 10%, 20%, 40% and 80%, respectively, followed by introducing an excess of water to make the aggregates become kinetically frozen, and then dialyzed against deionized water to remove DMF. The selectivity of water for PMAA allows the manipulation of interfacial curvature between the hydrophilic corona and hydrophobic core within a micelle, thus providing a means to control local micelle geometry. To explore this, we evaluated the micelle morphologies for the polymer as a function of water content.

Characterization

Molecular weights M_n and polydispersity index (PDI) M_w/M_n were determined by gel permeation chromatography (Waters
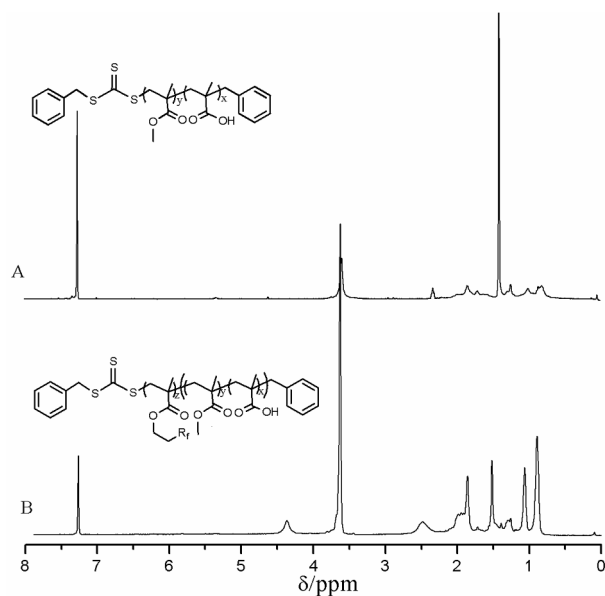
Fig. 1 ^{1}H NMR spectra of P(MMA-*co*-MAA) (A) and P(MMA-*co*-MAA)-*b*-PFEMA (B) in CDCl$_3$.

150C) (GPC) equipped with three Waters Styragel columns (10^3,
5 10^4 and 10^5 Å) and a refractive index detector (set at 35 °C),
using THF as an eluent at a flow rate of 1.0 mL min^{-1} at 35 °C
with polystyrene standards. Fourier transform infrared spectra
(FT-IR) were recorded on a Perkin-Elemer Spectrum one
spectrometer. Fluorine element analysis (F-EA) was used to
10 determine the fluorine content of the copolymer.[44] ^{1}H NMR
spectra were recorded on a 400 Hz NMR instrument
spectrometer, using CDCl$_3$ as the solvent and TMS as a reference
for chemical shifts. Dynamic light scattering (DLS) was
performed by a LLS spectrometer (ALV/CGS-5022) equipped
15 with an ALV-High QE APD detector and an ALV-5000 digital
correlator using a He-Ne laser (the wavelength λ=632.8 nm) as
the light source. The scattering data were recorded at 25 °C at a
scattering angle of 90°. The transmission electron microscopy
(TEM) observation was carried out on a JEM-1400 microscope
20 with an accelerating voltage of 200 kV.

Results and discussion

Synthesis of triphilic copolymer P(MMA-*co*-MAA)-*b*-PFEMA

As shown in Scheme 1, the triphilic block copolymer was
synthesized by the RAFT polymerization. The chain transfer
25 agent used was DBTTC, which was verified to have a well
controllability for the polymerization of acrylate.[45] Fig. 1A
depicts the ^{1}H NMR spectrum of P(MMA-*co*-PMAA) in CDCl$_3$.
The signals at 0.83-1.43 ppm are assigned to the protons of the
methyl groups (-C-C*H$_3$*) originating from PMMA and PMAA.
30 The signals at 1.70-1.87 ppm are assigned to the protons of the
methylene groups (-C*H$_2$*-) from the main chain, and the peak at
3.6 ppm is attributed to the protons of methoxyl group (-OC*H$_3$*)
from PMMA. Compared with the ^{1}H NMR spectrum of P(MMA-
co-PMAA) (Fig. 1A), the new signals (Fig. 1B) at 4.36 ppm are
35 assigned to the protons of methylene group (-O-C*H$_2$*-) in PFEMA
and the signals at 2.47 ppm (Fig. 1B) are attributed to the protons
of methylene group adjacent to the perfluoroalkyl group (-C*H$_2$*-R$_f$
), indicating that the fluorinated blocks have been introduced
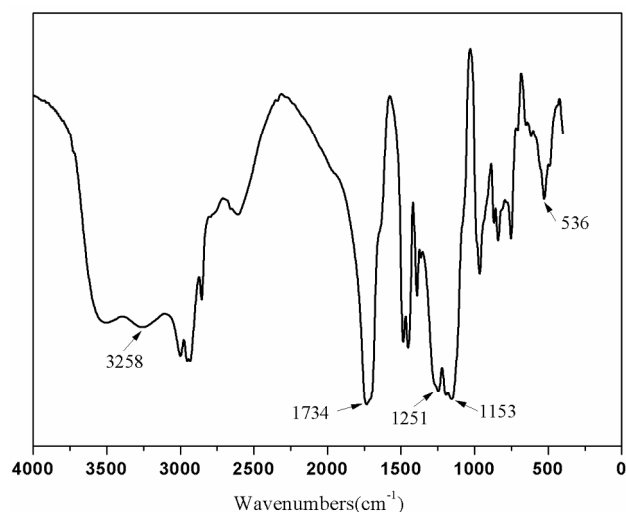

40 **Fig. 2** FT-IR spectra of P(MMA-*co*-MAA)-*b*-PFEMA.

Table 1 Characterization of the synthesized polymers

sample	$M_n(\times10^4\,\text{g mol}^{-1})$	PDI[a]	F(wt%)[b]	DP$_F$[c]
P(MMA-*co*-MAA)	3.89[a]	1.89	--	--
P(MMA-*co*-MAA)-*b*-PFEMA	4.28[d]	--	9.1	6.5

[a] Determined by GPC in THF with calibrated PS standards at 35 °C.
[b] Determined by F-EA.
[c] Degree of polymerization of FEMA, calculated based on the following
equation:F% = (DP$_F$ × 17.88 × 19)/{$M_{\text{n P(MMA}-co-\text{PMAA)}}$ + DP$_F$ × 554},
45 17.88 is the average number of fluorine atoms, 19 is therelative atomic
weight of fluorine atoms, 554 is the averagemolecularweight of FEMA.
[d] Calculated based on the following equation:
$M_{\text{n P(MMA}-co-\text{PMAA)}-b-\text{PFEMA}}$ = $M_{\text{n P(MMA}-co-\text{PMAA)}}$ + DP$_F$ × 554.

into the copolymer.

50 The FT-IR measurements were carried out to further confirm
the structure of resultant polymer P(MMA-*co*-MAA)-*b*-PFEMA.
As shown in Fig. 2, the appearance of an absorption at 3258 cm^{-1}
should be assigned to the vibration frequency of the carboxylic
acid group (-COOH), which suggested that the MAA was
55 incorporated into copolymer successfully. The absorption at 1734
cm^{-1} corresponding to the vibration frequency of the ester bond
(C=O), the signals at 1251-1153 cm^{-1} correspond to the
antisymmetric and symmetric stretching vibrations of the -CF$_3$
group, respectively, and signals at 536 cm^{-1} correspond to a
60 combination of the cocking and wagging vibrations of the -CF$_2$
group.

The M_n and PDI of P(MMA-*co*-MAA) copolymer were
measured by the GPC in tetrahydrofuran (THF) and the results
are presented in Table 1. However, due to the special solubility of
65 FEMA, the fluorinated block copolymer P(MMA-*co*-MAA)-*b*-
PFEMA tends to associate in THF even at very low
concentrations, which hampered its meaningful molecular weight
analysis by GPC. Hence, we used fluorine element analysis as
well as the molecular weight of the macroinitiator to determine
70 the molecular weight of resultant copolymer and the fluorine
content.[44] The calculation method in detail can be found in the
annotation of Table 1. The properties of the copolymer were
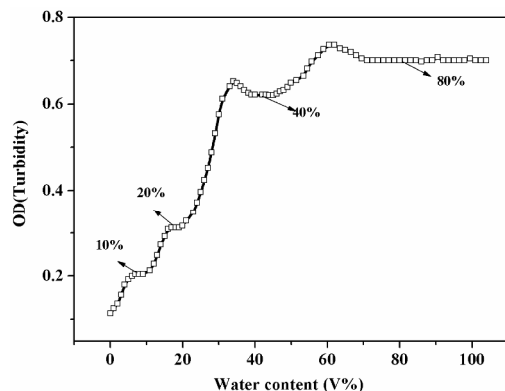shown in Table 1.

Fig. 3 Turbidity (optical density) curves of the triphilic copolymer solution in DMF at an initial concentration of 1.0 g L^{-1} as a function of an amount of water added to the solution.

Turbidity measurements (OD)

UV absorption value of the solution changes with the size, amount and morphology of aggregates in solution.[46] Therefore, the measurement of absorbance is an effective tracking method for the polymer micelle formation process. Fig. 3 shows the diagrams of UV absorbance versus water content of the solutions at an initial copolymer concentration of 1.0 g L^{-1}. Changes of the UV absorbance reflect changes of the aggregates in the solutions. With the introduction of the water, the copolymer chains tend to aggregate due to the hydrophobicity of PMMA and PFEMA blocks and the number of aggregates is increased, so the absorbance became larger. The platform indicated the status of micelles in a relatively stable state. Such a change of turbidity is relative to the process of the self-assembly of triphilic copolymers, where the intermediate structures or the various aggregation structures may be formed or coexisted during addition of water.[47, 48] There are four platforms in Fig. 3, and it is in accordance with the four different morphologies. The details would be discussed in the following sections.

Self-assembly behavior of triphilic copolymer P(MMA-*co*-MAA)-*b*-PFEMA in solution

Block copolymer self-assembly is a powerful strategy to access a variety of nanostructures via mild processing conditions.[14, 49-51] Intra and inter-molecular attractive and repulsive forces can be precisely tuned by the chemical composition of the constituent blocks and solution conditions. Aqueous self-assembly of block copolymer was conducted by first dissolving the polymer in DMF, followed by solvent exchange with water by dialysis. Water, a poor solvent for the PMMA and PFEMA blocks, drives the self-assembly due to the hydrophobicity of the core-forming blocks, while the nanostructures are stabilized by the water-soluble PMAA segments. The self-assembled structures and morphologies were investigated by the combination of TEM and DLS.

In Fig. 4, a novel nanostructure were observed, which changed from spheres and short worms (Fig. 4A) to wormlike structures (Fig. 4B), to tapered worms (Fig. 4C), finally to nail-shaped structures (Fig. 4D), as the WC increased from 10% to 80%. It is accordance with turbidity curve in Fig. 3, which showed four narrow platforms before the WC reached 80%. The addition of water has the combined effect of aggregating the hydrophobic
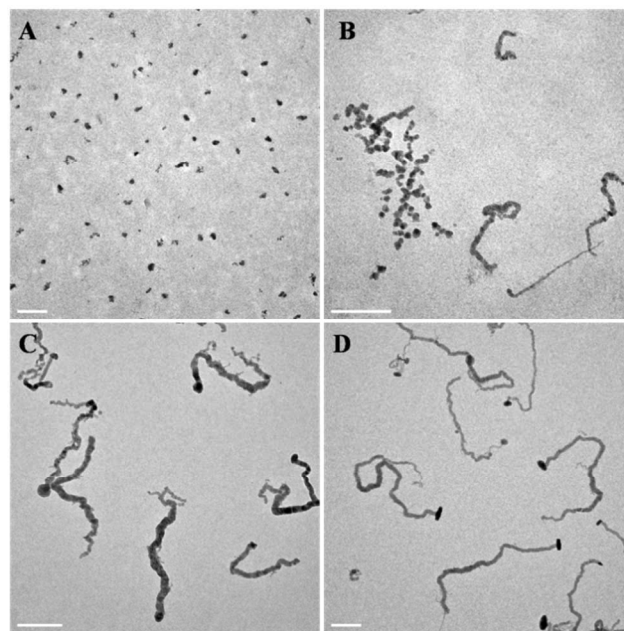

Fig. 4 TEM images of P(MMA-*co*-MAA)-*b*-PFMA micelle structural evolution with the addition of water: (A) WC-10%; (B) WC-20%; (C) WC-40%; (D) WC-80%. The scale bar is 200 nm.
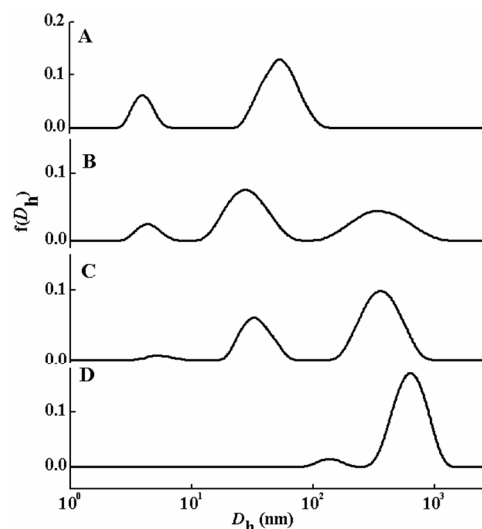

Fig. 5 D_h distribution by DLS at a scattering angle of 90°: (A) WC-10%; (B) WC-20%, (C) WC-40%; (D) WC-80%.

PMMA and PFEMA blocks while concurrently swelling and eventually solubilizing the PMAA segments into micelle corona, and resulted in increasing of interfacial energy and internal phase separation between PMMA and PFEMA, producing wormlike micelles with uneven diameters and variable morphology (Fig. 4).

In WC-10%, the spheres and short worms were obtained, as shown in Fig. 4A. The aggregates have a diameter ranging from 25 to 40 nm and the lengths are ranged from 40 to 100 nm. The size measured by using TEM appears smaller than the average size calculated from DLS (Fig. 5A) because of the collapse of the well-solubilized corona during the TEM sample preparation.

The aggregation structures at WC of 20% are shown in Fig. 4B, the mixture of spheres, short worms and long wormlike micelles were obtained. The wormlike micelles had different

lengths ranging from 100 to 500 nm. Apparently, the spheres and short worms tended to aggregate (see Fig. S1 in ESI), and the worms had a rough surface, suggesting that the wormlike micelles derive from the spheres. The cluster behaviour of spheres was due to the interplay of interfacial energy minimization and entropy maximization. The DLS result was shown in Fig. 5B. There are two main peaks. One was located at 30 nm with a population of 50.6%, which was attributed to the spheres. The other peak with a population of 40.4% had an average diameter of 389 nm contributed to the wormlike micelles.

For WC-40%, tapered micelles with length beyond one micrometre were observed (Fig. 4C). There were variations in diameters of the structures. The large end had a diameter ranging from 20 to 50 nm, while the small end exhibited diameters around 5-10 nm. The surface morphology was much smoother than that of WC-20%. The DLS results also indicated that more spheres were organized into wormlike aggregates with the addition of water. In Fig. 5C, the peak locating around 30 nm represent 33.4% of the population were much less than the number 50.6% in the sample of WC-20%. Certainly, the population of wormlike micelles also increased, from 40.4% to 66.5%.

When more water was added, WC reached 80%. TEM results show that wormlike aggregates extend more than one micrometer and exhibit uneven diameters and end caps (Fig. 4D). Compared to the tapered micelle in WC-40%, these structures were much longer and there were also some hairs along the micelles, and were similar to the shape of nail. DLS results for these novel nail-shaped worms demonstrated a distribution of populations with a hydrodynamic diameter (D_h) of 647 nm on average, representing 94.7% of the population, as shown in Fig. 5D.

DLS results in Fig. 5 demonstrated that more spheres and short worms were organized into long wormlike aggregates with the addition of water. The population of the spheres and short worms with size blow 200 nm was eventually decreased, and correspondingly, the number of long worms with the size ranged from 200 to 1000 nm was increased. By comparing D_h of the main population in aqueous media with lengths of those structures showing curled shapes in TEM (Fig. 4B, C, D), the size of the particles in aqueous solution was less than the lengths obtained from TEM images. We conclude that the wormlike structures behave as coils in water.

The aggregate morphology is determined primarily by a force balance among three contributions: the core-chain stretching, corona-chain repulsion and interfacial tension between the core and the outside solution.[52] Consequently, factors that influence the above balance can be used to control the aggregate architecture. It was shown that the shape, as well as the size of the aggregates depends not only on polymer related properties, such as the relative block length or the polydispersity of polymer blocks, but also, and to a greater extent, on the solution conditions.[53] The ability to induce a series of morphological transitions by adding water can be explained in terms of the effect of water content on the three factors that govern the aggregate morphology: the core-chain stretching, corona-chain repulsion and interfacial tension.

The solvent-dependent particle sizes can be rationalized by solvent quality/polarity, i.e., water is a more polar solvent than DMF. Hence the interfacial tension between the core-forming block (PMMA and PFEMA) and solvent will be increased with the continuous increase of the water content. In response to this increase, the system tends to decrease the total interfacial area by increasing the micellar size (i.e., by increasing the aggregation number) while reducing the total number of aggregates,[54] this behaviour results in the micelle fusion. Just as the DLS results (Fig. 5) show that the number of wormlike micelles increases accompanied by the decrease of the population of the mixture of spheres and short worms with the water addition. However, the increase in the micellar dimension is accompanied by the thermodynamically unfavorable increase in core-chain stretching and corona chain repulsion. When the thermodynamic penalty due to these factors exceeds the driving force to reduce the interfacial area, and in order to reduce the total free energy of the system, the spheres undergo a morphological transition into smaller-diameter wormlike structures with the WC increase from 10% to 20% (Fig. 4A, B), whereby the core-chain stretching and the inter-coronal repulsion are reduced.

Studies on block copolymer aggregates also verified a series of morphological transitions were occurred by control the solution conditions.[49, 55, 56] In our case, the fusion processes by virtue of spheres and short worms transform into long worms were first occurred, further slow intra-micelle segregation leads the formation of nail-shaped structure with uneven diameter along the axis of the worms.

To understand the mechanism for forming the asymmetrical structures, one should bear in mind that the polymer P(MMA-*co*-MAA)-*b*-PFEMA we used was a triphilic copolymer with special structure. The amphiphilic random copolymer P(MMA-*co*-MAA) was first synthesized as the macroinitiator, followed by incorporating the fluorophilic block PFEMA, which is well-defined. What's more, the polymer chains have variable carboxyl content. That is to say, some were incorporated more PMAA segments, others less. The asymmetrical distribution of the hydrophilic segments depends, in great part, on the nature of the random blocks. And the polydispersity of the random copolymer, which is reached at 1.89, also plays an important role in the chemical heterogeneity. Both the high PDI and the nature of the random copolymer have a significant effect on the distribution of PMAA segments, which can further lead to form the asymmetrical structures, which may affect the nature of morphologies formed in aqueous media, and account for the unusual self-assembly behaviour resulting in complex morphologies.

The most important factor leading the formation of the uneven-diameter worms is interfacial energy between the core and the solvent, which is between PFEMA and PMAA/H_2O in our case. Increasing interfacial energy would drive chains to stretch away from the interface with preferential formation of flat interface, finally leading to domain size expansion.[57] As a result, the extent that the chains stretch depends on interfacial tension. Obviously, there are very close relationship between interfacial tension and hydrophilic block, the more PMAA segments on polymer chains, and the higher interfacial energy between core and corona. The larger-diameter regions within the worms are considered to be regions that are concentrated in polymer chains with more PMAA segments. Because there is a higher interfacial energy between PFEMA and blocks with more PMAA, relative to chains with

less PMAA, causing more chain stretching so as to limit PFEMA interactions with surrounding lipophilic blocks PMMA. Mays *et al.*[32] reported that tapered rods were obtained from fluorinated and partly sulfonated copolymer (*s*PS-*b*-*f*PI), as a result of *f*PI chains stretching to various extension levels, which drive forced by the sulfonation degree of PS block. Substantial stretching of core chains at the large end of the rods is caused by strong stretching of sulfonated PS blocks with high sulfonation degree. It is in accordance with above analysis. It also has reported that a higher interfacial energy for a triblock copolymer containing poly(pentafluorostyrene) (PPFS) caused intra-micellar phase separation and, more importantly, the undulation of cylindrical assembly due to more stretching from the PPFS block.[49] On the other hand, copolymers with fluorinated and nonfluorinated blocks are known to undergo strong phase segregation in solution because of the unique solubility characteristics of fluorinated structures.[58, 59] And in our case, there are stronger incompatibility between the fluorophilic blocks PFEMA and the blocks P(MMA-*co*-MAA) with more PMAA segments, which lead to higher degree of intra-micellar phase separation and induce larger diameter. In fact, the segregation behaviour of the core-forming blocks PFEMA is in agreement with theoretical predictions by Semenov *et al.*[60, 61] who identified a new regime of phase behaviour that they dubbed "superstrong segregation". In this regime, the repulsive interactions between two adjoining blocks become so strong that the interfacial energy overwhelms the conformational entropy or coronal crowding, as such, the minor block becomes nearly stretched out completely.[60]

Interesting, a unique morphology was observed (see Fig 4D and Fig. S2 in ESI). The nail-shaped micelles were evolved from the asymmetrical worms as the water content increasing from 40% to 80%. In this process, the interfacial tension between the core-forming blocks and solvent will increase and it is also accompanied by the entropic penalties. In order to minimize the total free energy, the intra-micelle segregation occurred. This segregation behaviour is reinforced by the highly incompatibility between fluorocarbons and hydrocarbons. The combined effects induced the evolution of the micellar shape. So we propose that the "head" of the nail-shaped micelles appeared as dark in TEM images (Fig. 4 D) corresponds to PFEMA-rich domains. Similar colour contrast in TEM images without staining, which was induced by phase separation between the lipophilic and fluorophilic segments, was also observed by some researchers.[12, 37] Further research is required to explore the formation mechanism, as well as verify the composition of the "head" of the nail-shaped micelles.

Conclusion

A novel fluorinated triphilic copolymer has been synthesized by two successive RAFT polymerizations. The structural evolution of P(MMA-*co*-MAA)-*b*-PFEMA micelles in the mixtures of DMF and H_2O was investigated. It showed that the "triphilic" copolymer self-assembled into novel nail-shaped structures in dilute aqueous solutions. In mixtures of DMF and H_2O, results consistently indicate that the structures formed by P(MMA-*co*-MAA)-*b*-PFEMA evolve from spheres and short worms to nail-shaped worms as H_2O content increases. DLS measurements also have been done to confirm the aggregate transition. The micelle morphology evolves upon addition of H_2O due to the increasing of the interfacial tension between the core-forming block and solvent. Collectively, these results demonstrate how micelle structure evolves and can be controlled by controlling solvent composition and polymer structure.

Acknowledgements

References

1. K. Kataoka, A. Harada and Y. Nagasaki, *Adv. Drug Del. Rev.*, 2012, **64**, 37-48.

2. M. S. Aw, M. Kurian and D. Losic, *Chem.-Eur. J.*, 2013, **19**, 12586-12601.

3. H. Wei, R.-X. Zhuo and X.-Z. Zhang, *Prog. Polym. Sci.*, 2013, **38**, 503-535.

4. J. Babinot, E. Renard, B. Le Droumaguet, J.-M. Guigner, S. Mura, J. Nicolas, P. Couvreur and V. Langlois, *Macromol. Rapid Commun.*, 2013, **34**, 362-368.

5. A. M. Nystrom, J. W. Bartels, W. Du and K. L. Wooley, *J. Polym. Sci., Part A: Polym. Phys.*, 2009, **47**, 1023-1037.

6. E. Amado and J. Kressler, *Soft Matter*, 2011, **7**, 7144-7149.

7. S. O. Kyeremateng, E. Amado, A. Blume and J. Kressler, *Macromol. Rapid Commun.*, 2008, **29**, 1140-1146.

8. A. O. Moughton, T. Sagawa, W. M. Gramlich, M. Seo, T. P. Lodge and M. A. Hillmyer, *Polym. Chem.*, 2013, **4**, 166-173.

9. K. Skrabania, H. von Berlepsch, C. Boettcher and A. Laschewsky, *Macromolecules*, 2010, **43**, 271-281.

10. Y. Patil and B. Ameduri, *Prog. Polym. Sci.*, 2013, **38**, 703-739.

11. T. P. Lodge, J. A. Bang, Z. B. Li, M. A. Hillmyer and Y. Talmon, *Faraday Discuss.*, 2005, **128**, 1-12.

12. J.-N. Marsat, M. Heydenreich, E. Kleinpeter, H. V. Berlepsch, C. Boettcher and A. Laschewsky, *Macromolecules*, 2011, **44**, 2092-2105.

13. J.-N. Marsat, F. Stahlhut, A. Laschewsky, H. v Berlepsch and C. Boettcher, *Colloid. Polym. Sci.*, 2013, **291**, 2561-2567.

14. Z. B. Li, E. Kesselman, Y. Talmon, M. A. Hillmyer and T. P. Lodge, *Science*, 2004, **306**, 98-101.

15. Z. Li, M. A. Hillmyer and T. P. Lodge, *Langmuir*, 2006, **22**, 9409-9417.

16. S. Kubowicz, J. F. Baussard, J. F. Lutz, A. F. Thunemann, H. von Berlepsch and A. Laschewsky, *Angew. Chem. Int. Ed.*, 2005, **44**, 5262-5265.

17. C. Liu, M. A. Hillmyer and T. P. Lodge, *Langmuir*, 2008, **24**, 12001-12009.

18. A. O. Moughton, M. A. Hillmyer and T. P. Lodge, *Macromolecules*, 2012, **45**, 2-19.

19. J.-F. Gohy, N. Lefevre, C. D'Haese, S. Hoeppener, U. S. Schubert, G. Kostov and B. Ameduri, *Polym. Chem.*, 2011, **2**, 328-332.

20. H. Von Berlepsch, C. Boettcher, K. Skrabania and A. Laschewsky, *Chem. Commun.*, 2009, DOI: 10.1039/b903658j, 2290-2292.

21. K. Skrabania, A. Laschewsky, H. v. Berlepsch and C. Boettcher, *Langmuir*, 2009, **25**, 7594-7601.

22. B. Fang, A. Walther, A. Wolf, Y. Xu, J. Yuan and A. H. Muller, *Angew. Chem. Int. Ed.*, 2009, **48**, 2877-2880.

23. L. F. Zhang. and A. Eisenberg, *J. Am. Chem. Soc.*, 1996, **118**, 3168-3181.

24. S. J. Holder and N. A. J. M. Sommerdijk, *Polym. Chem.*, 2011, **2**, 1018-1028.

25. M. Lobert, R. Hoogenboom, C.-A. Fustin, J.-F. Gohy and U. S. Schubert, *J. Polym. Sci., Part A: Polym. Phys.*, 2008, **46**, 5859-5868.

26. B. H. Tan, H. Hussain, Y. Liu, C. B. He and T. P. Davis, *Langmuir*, 2010, **26**, 2361-2368.

27. H. W. Shen and A. Eisenberg, *Macromolecules*, 2000, **33**, 2561-2572.

28. X. Y. Liu, J. Wu, J. S. Kim and A. Eisenberg, *Langmuir*, 2006, **22**, 419-424.

29. P. Tanner, P. Baumann, R. Enea, O. Onaca, C. Palivan and W. Meier, *Acc. Chem. Res.*, 2011, **44**, 1039-1049.

30. B. H. Tan, H. Hussain, K. C. Chaw, G. H. Dickinson, C. S. Gudipati, W. R. Birch, S. L. M. Teo, C. He, Y. Liu and T. P. Davis, *Polym. Chem.*, 2010, **1**, 276-279.

31. T. P. Lodge, A. Rasdal, Z. B. Li and M. A. Hillmyer, *J. Am. Chem. Soc.*, 2005, **127**, 17608-17609.

32. X. Wang, K. Hong, D. Baskaran, M. Goswami, B. Sumpter and J. Mays, *Soft Matter*, 2011, **7**, 7960.

33. A. F. Thunemann, S. Kubowicz, H. von Berlepsch and H. Mohwald, *Langmuir*, 2006, **22**, 2506-2510.

34. D. Liu and C. Zhong, *Macromol. Rapid Commun.*, 2007, **28**, 292-297.

35. J. Xia, D. Liu and C. Zhong, *PCCP*, 2007, **9**, 5267.

36. Y. Gao, X. Li, L. Hong and G. Liu, *Macromolecules*, 2012, **45**, 1321-1330.

37. S. O. Kyeremateng, K. Busse, J. Kohlbrecher and J. Kressler, *Macromolecules*, 2011, **44**, 583-593.

38. Z. B. Li, M. A. Hillmyer and T. P. Lodge, *Macromolecules*, 2004, **37**, 8933-8940.

39. Z. B. Li, M. A. Hillmyer and T. P. Lodge, *Nano Lett.*, 2006, **6**, 1245-1249.

40. Z. L. Zhou, Z. B. Li, Y. Ren, M. A. Hillmyer and T. P. Lodge, *J. Am. Chem. Soc.*, 2003, **125**, 10182-10183.

41. A. Laschewsky, *Curr. Opin. Colloid Interface Sci.*, 2003, **8**, 274-281.

42. R. K. Bai, Y. Z. You and C. Y. Pan, *Macromol. Rapid Commun.*, 2001, **22**, 315-319.

43. J. Zipfel, J. Berghausen, G. Schmidt, P. Lindner, P. Alexandridis and W. Richtering, *Macromolecules*, 2002, **35**, 4064-4074.

44. X. X. Li, B. Fang, S. Lin, P. P. Wu and Z. W. Han, *Acta Polymeric Sinica*, 2003, **6**, 910-913.

45. Y. Z. You, C. Y. Hong, R. K. Bai, C. Y. Pan and J. Wang, *Macromol. Chem. Phys.*, 2002, **203**, 477-483.

46. Y. Wang, S. Lin, M. Zang, Y. Xing, X. He, J. Lin and T. Chen, *Soft Matter*, 2012, **8**, 3131.

47. G. Yu and A. Eisenberg, *Macromolecules*, 1998, **31**, 5546-5549.

48. J. Yang, R. Pinol, F. Gubellini, D. Levy, P.-A. Albouy, P. Keller and M.-H. Li, *Langmuir*, 2006, **22**, 7907-7911.

49. H. Cui, Z. Chen, S. Zhong, K. L. Wooley and D. J. Pochan, *Science*, 2007, **317**, 647-650.

50. A. H. Groeschel, F. H. Schacher, H. Schmalz, O. V. Borisov, E. B. Zhulina, A. Walther and A. H. E. Mueller, *Nat Commun.*, 2012, **3**, 1-10.

51. R. C. Hayward and D. J. Pochan, *Macromolecules*, 2010, **43**, 3577-3584.

52. Lifeng Zhang and A. Eisenberg*, *Polym. Adv. Technol.*, 1998, **9**, 677-699.

53. A. Choucair and A. Eisenberg, *Eur. Phys. J. E.*, 2003, **10**, 37-44.

54. H. W. Shen and A. Eisenberg, *J. Phys. Chem. B*, 1999, **103**, 9473-9487.

55. C.-W. Wang, D. Sinton and M. G. Moffitt, *Acs Nano*, 2013, **7**, 1424-1436.

56. J. G. Ray, A. J. Johnson and D. A. Savin, *J. Polym. Sci., Part B: Polym. Phys.*, 2013, **51**, 508-523.

57. M. W. Matsen and F. S. Bates, *J. Chem. Phys.*, 1997, **106**, 2436-2448.

58. H. Shimomoto, D. Fukami, S. Kanaoka and S. Aoshima, *J. Polym. Sci., Part A: Polym. Phys.*, 2011, **49**, 2051-2058.

59. K. Matsumoto, H. Mazaki and H. Matsuoka, *Macromolecules*, 2004, **37**, 2256-2267.

60. A. N. Semenov, I. A. Nyrkova and A. R. Khokhlov, *Macromolecules*, 1995, **28**, 7491–7500.

61. I. A. Nyrkova., A. R. Khokhlov. and M. Doi., *Macromolecules*, 1993, **26**, 3601–3610.

Graphical Abstract

Synthesis and Self-Assembly of a Novel Fluorinated Triphilic Block Copolymer

Xinxin Li*[a], Yanhua Yang[a], Guojun Li[a] and Shaoliang Lin*[ab]
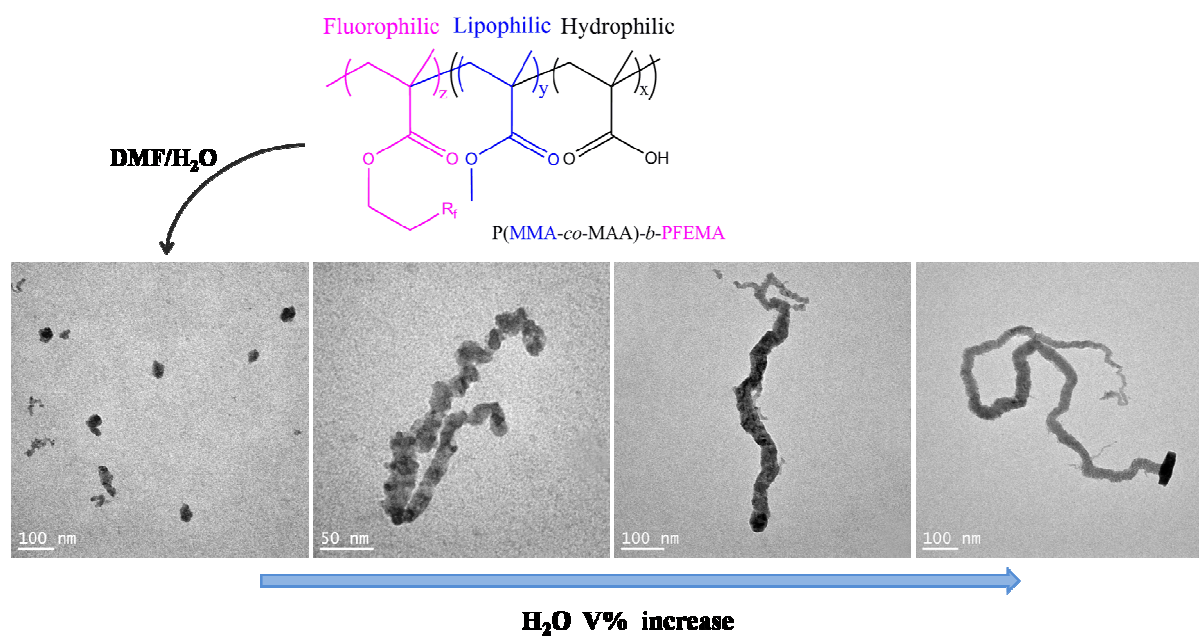
The morphology evolution of triphilic copolymer P(MMA-co-MAA)-b-PFEMA aggregates self-assembled in DMF/H_2O solutions with the increase of water content.